IEEE Access
Multidisciplinary | Rapid Review | Open Access Journal

Received April 21, 2017, accepted May 16, 2017, date of publication May 26, 2017, date of current version July 3, 2017.

Digital Object Identifier 10.1109/ACCESS.2017.2707560

Measurement and Modeling of Wireless Off-Body Propagation Characteristics Under Hospital Environment at 6-8.5 GHz

PENG-FEI CUI, YU YU, WEN-JUN LU, (Member, IEEE), YANG LIU, AND HONG-BO ZHU
Jiangsu Key Laboratory of Wireless Communications, Nanjing University of Posts and Telecommunications, Nanjing 210003, China

Corresponding author: Peng-Fei Cui (1203883589@qq.com)

This work was supported in part by the National Natural Science Foundation Council Proposal under Grant 61427801 and Grant 61471204 and in part by the Jiangsu Scientific Innovation Research of University Graduate under Grant KYLX16_0657.

ABSTRACT A measurement-based novel statistical path-loss model with a height-dependent factor and a body obstruction (BO) attenuation factor for off-body channel under a hospital environment at 6–8.5 GHz is proposed. The height-dependent factor is introduced to emulate different access point (AP) arrangement scenarios, and the BO factor is employed to describe the effect caused by different body-worn positions. The height-dependent path-loss exponent is validated to fluctuate from 2 to 4 with AP height increasing by employing both computer simulation and classical two-ray model theory. As further validated, the proposed model can provide more flexibility and higher accuracy compared with its existing counterparts. The presented channel model is expected to provide wireless link budget estimation and to further develop the physical layer algorithms for body-centric communication systems under hospital environments.

INDEX TERMS Body-centric communication (BCC), height-dependent, path-loss exponent, off-body, body obstruction, hospital.

I. INTRODUCTION

The capacity boosting, ultra reliability and massive connectivity are key technologies of the 5th Generation (5G) mobile communications. In order to accomplish these techniques, it is necessary to extend the future mobile communications to more frequency bands. It is pointed out that the international mobile telecommunication (IMT) has at least a 663 MHz spectrum deficit [1]. Whilst, the super high frequency (SHF) bands, especially the 5-10 GHz, provides a promising choice for such a frequency deficit. Further, the SHF band has great potential to realize the 5G key performance indicators, such as up to 1 GBps cell edge user data rate and 1000 times traffic density [2]. Thus, it is critical to fully investigate the propagation characteristics of the SHF band to provide robust wireless coverage and to develop robust physical layer transmission schemes.

People's increasing need to communicate at anytime and anywhere in 5G era has promoted the development of body-centric communication (BCC) as they allow for the integration of wearable and/or hand-held devices within the surrounding infrastructure [3]. According to the mutual position of the transmitter (Tx) and receiver (Rx) involved in the body-centric transmission, it is possible to identify four communication scenarios: In-body, On-body, Off-body and Body-to-Body [4]. In these scenarios, the off-body scenario causes increasing attention in both academia and industry for the function of direct access to the Internet.

The off-body channel is characterized by on-body wearable devices access to remote access point (AP). The propagation characteristics of off-body channel are considered to be mainly dependent on four factors including the antenna body-worn locations [5], AP deployment [3], body posture (including both static and dynamic scenarios) [3], [6] and carrier frequency [3], [7], [8]. Compare to the widely reported off-body channel characteristics under walking and body-rotation states [3], [5], the propagation characteristics under lying state is rarely studied [9]. Since the successful application of height gain factor of Okumura model [10], a large number of AP height dependent path loss studies under cellular communications are reported [11], [12]. Although the IEEE 802.15 (Channel Model for Body Area Network (BAN) 8.2.10.B.A) views the impact of antenna height as the primary channel factor for off-body communication (body surface to external) [13], the impact of AP height on path loss exponent (PLE) in off-body channel is seldom studied. There are a large number of statistical analyses of different body-worn

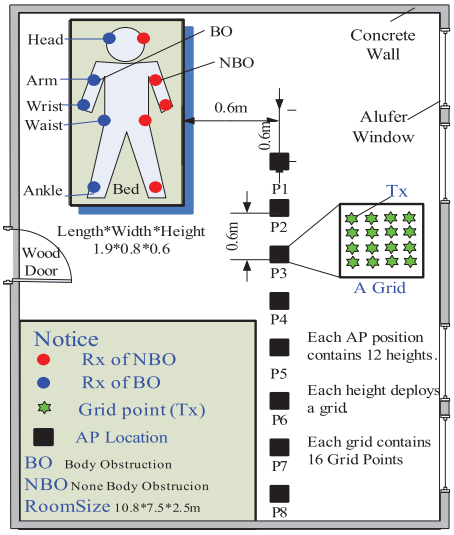

FIGURE 1. Illustration of the typical hospital scenario with definite measurement locations (External AP functions as Tx).

links and various body postures [3], [5]–[8]. Nevertheless, few statistics are used to set up a synthetically path-loss model. Thus, it is of critical concern for the BCC system to build an off-body path-loss model which systematically takes body-worn locations, AP emplacement and statistical influences into consideration under lying state. Furthermore, it would be useful to describe the small scale fading features, such as time delay dispersion, multi-path components distributions, coherence bandwidth etc. [14], [15].

In this paper, a novel off-body propagation model with a height-dependent PLE factor and a body obstruction (BO) factor is studied. Section II presents the measurement campaign. Section III depicts the details of the proposed dual-factor model. The experimental simulation and validation is introduced in Section IV. To the best of the authors' knowledge, this is the first path-loss model that can describe the effects of variable antenna-height and body-worn-location deployments. As the dual factors provide clear physical insights into the transmitter and receiver conditions, the proposed model can be flexibly implemented in engineering and beneficial to the theoretical exploration. With the computer simulation, it exhibits higher accuracy than the conventional models.

II. CHANNEL MEASUREMENT

A. MEASUREMENT SETUP AND SCHEMES

Measurement campaign is conducted in a typical less-furniture, hospital room environment shown in Fig. 1. An omnidirectional monopole antenna is used to emulate the external access point (AP) shown on the left in Fig. 2(a), and a wearable loop-dipole combined antenna worn on different positions of the volunteer is used to emulate the receiver (Rx) [16]. The measured radiation pattern of the wearable antenna is shown in Fig. 2(b) and Fig. 2(c) and the antenna gains are removed from the path loss during the data analysis. Due to the high cross-polarization of the RX antenna

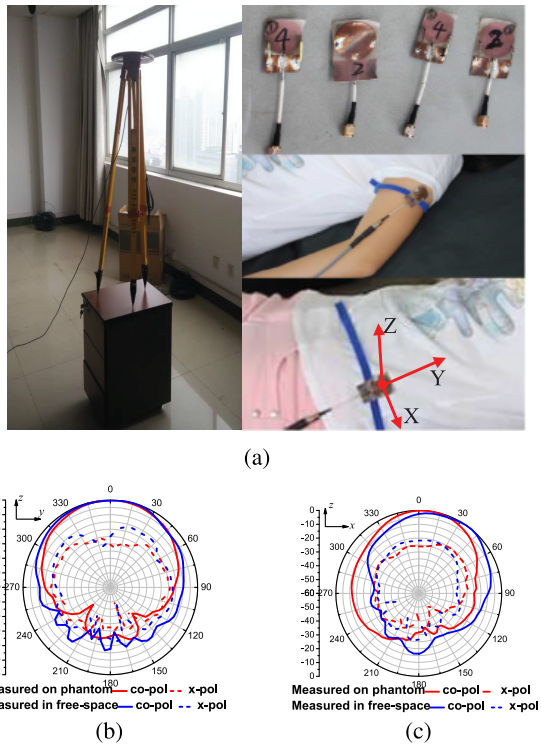

FIGURE 2. The illusion of (a) Real environment and equipment and radiation pattern for the wearable antenna in (b) E-plane and (c) H-plane.

and the scattering around the lying body, the polarization mismatch has no significant effect on the signal measurement. A vector network analyzer (cf. VNA Agilent 8720) is used to generate a 0 dBm, 801-point sweeping signal with the frequency ranging from 6 to 8.5 GHz. The measured data are stored in a laptop computer via a general purpose interface bus (GPIB) interface. Table 1 shows the parameters for the measurement system and more details can be found in [17]–[20].

In order to study the influence of AP height and body-worn position on the off-body channel, two schemes are designed: In scheme I, the external AP is deployed to 12 variable heights to study the relationship between the large scale fading and different AP heights. In scheme II, the wearable antenna is disposed to ten primary on-body positions, including the left and right side of head, arm, wrist, waist, and ankle to explore attenuations caused by alerted antenna body-worn positions [21]. Small scale features like time dispersion and multipath for ten antenna body-worn positions are further extracted to study the body obstruction effect. In the measurement, the volunteer keeps static. Therefore, the propagation channel under test is recognized as a non-time-variant channel so that its time dispersion characteristic can be measured by a VNA in frequency domain [22].

1) SCHEME I: LARGE-SCALE SCHEME WITH VARIABLE AP HEIGHT

When performing the height-dependent measurement campaign [17], [18], the wearable antenna (Rx) is fixed on

TABLE 1. Parameters of measurement system.

Parameter	Value
Center frequency	7.25 GHz
Bandwidth	2500 MHz
Frequency separation	3.125 MHz
Sweeping time	400 ms
Transmit power	0 dBm
Low noise amplifier	20 dB
Power amplifier	20 dB

the left wrist of the volunteer. The AP mounted atop a wooden tripod is alternatively deployed at 12 heights between 0.4 and 1.9 m. For each acquisition run, the AP equipment is sequentially placed at eight locations ranging from 0.8 to 5.0 m. In each location, the area is divided into 16 different points (44 matrix points) using a 5-cm spacing, as shown in Fig. 1.

2) SCHEME II: DIFFERENT ANTENNA BODY-WORN POSITIONS

Height of AP is fixed to 0.6 m, the same height as the hospital bed. To compare the BO and non-BO (NBO) effects, the wearable antenna is alternatively placed on five pairs of symmetrical on-body positions, i.e., the left and right side of head, arm, waist, wrist, and ankle in Fig.1. Six volunteers are tested with different physical characteristics (height, weight, and gender). Another two AP height, 0.4 m and 1.9 m are also measured for validation and comparison.

For both schemes, the measurement of each location is repeated five times to eliminate noise.

B. CLARIFICATION ON BO/NBO LEFT/RIGHT AND LOS/NLOS

Before channel modeling, three important concepts including NBO/BO, left/right side and Line Of Sight/ None Line Of Sight (LOS/NLOS) are illustrated to avoid possible confusion.

In our experiment, ten antenna body-worn positions are divided into two kinds of scenarios: BO and NBO. The former is defined that the direct link between wearable antenna and the AP is obstructed by human body, while the latter one is not.

For the off-body channel, BO is completely different from NLOS. LOS path between the AP and wearable antenna will not be completely blocked because the AP is higher than lying human in most BO cases. Similarly, NBO is not identical to the LOS scene, due to the complex antenna-body coupling effect, and the body shadowing effect that introducing extra attenuation. It is shown that the statistical signal level of the BO case is about 5dB larger than that of the NBO and the gap between BO and no body scene becomes even lager under the same emission conditions and environment [14].

As the direct link between AP and the wearable antenna on the left wrist in Fig. 1 is not obstructed by the volunteer in Scheme I, such scenario should be classified as the NBO case. However, if we take AP from the right side of the room to the left, the corresponding scenario would be changed, i.e., Scheme I would belong to the BO case. Thus, it is more convenient and reasonable to name such a scenario with the NBO wrist case than the traditional left wrist one.

III. DUAL-FACTOR PATH-LOSS MODEL

A. PROPOSED DUAL-FACTOR PATH-LOSS MODEL

Generally, average local path loss almost linearly increases with the logarithm of the Tx-Rx distance [23]. In order to describe the extra attenuation caused by the variations of the AP height and the antenna body-worn position, two factors are used to construct the proposed off-body path loss model. A height-dependent PLE factor is adopted to describe the influence of the AP height, and a body obstruction factor is added to describe the effects of different antenna body-worn positions. Then, the proposed novel dual-factor path loss model is represented by

$$PL(d) = PL(d_0) + 10N(h) \times log_{10}(\frac{d}{d_0}) + BOF + X_\delta \quad (1)$$

where the $PL(d)$ is the off-body path-loss value at the Tx-Rx separation distance d, $PL(d_0)$ is the measured path loss at the reference distance d_0, the $N(h)$ is the AP height-dependent PLE factor. The BOF is the extra body obstruction factor which is dependent on specific antenna body-worn position. The X_δ represents the shadowing effect which is a zero mean Gaussian random variable.

B. EXPRESSION OF AP HEIGHT-DEPENDENT PLE FACTOR

The AP height-dependent PLE factor is modeled as a quadratic function: [11]

$$N(h) = a \times h^2 + b \times h + c \quad (2)$$

where h represents the height of AP, const values a, b, c are three parameters of quadratic function which are dependent on the specific environment.

C. DESCRIPTION OF THE BODY OBSTRUCTION FACTOR

Based on the statistical parameters of the measurement results in Scheme II, the body obstruction factor which is dependent on specific antenna body-worn position is added to modify the attenuation caused by the body obstruction. As the observed data of ten body-worn cases all fit the log-normal distribution well, the BOF is represented by the statistical mean parameter of the log-normal model. Table 2 shows the normalized measurement-based BOF values by subtracting the reference value (i.e., the NBO case with Rx on the left wrist).

The theoretical derivation for PLE factor and BO factor would be described in Section IV.

TABLE 2. Measurement-based body obstruction factor under hospital environment.

BOF [dB]	Different Antenna Body-Worn Positions				
	Ankle	Wrist	Waist	Arm	Head
NBO category	-2.4	0.0	-4.9	-0.4	1.5
BO category	5.4	0.1	3.4	5.1	5.3

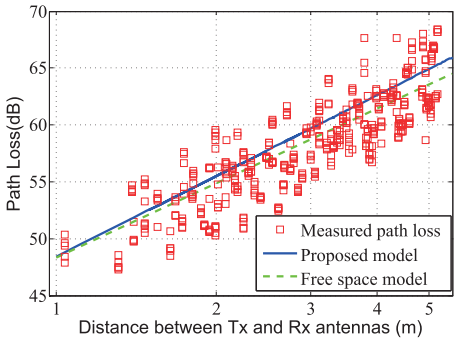

FIGURE 3. Scatter plots of the measured path loss values and the fitted curves.

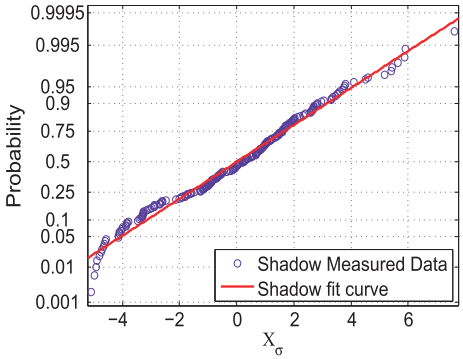

FIGURE 4. Probability plot of the shadow fading component X_δ in a typical bed-ward at 6-8.5 GHz.

TABLE 3. Basic parameters and path loss exponent factor function for proposed path loss model.

Para -meter	BASIC PARAMETERS			PLE Function $N(h)$		
	$PL(d_0)$ $[dB]$	General PLE	X_δ $[dB]$	a	b	c
Value	48.6	2.36	2.4	1.33	-2.64	3.52

IV. MODELING AND VALIDATION

A. PARAMETERS FOR PROPOSED PATH-LOSS MODEL

By averaging the complex frequency response data [24], [25], local path loss equation is calculated as following:

$$PL(d) = \frac{1}{MN}\sum_{i=1}^{M}\sum_{j=1}^{N}|H\left(f_i, t_j; d, h\right)|^2 - g_{ant}(\theta, \varphi) \quad (3)$$

where $H(f_i, t_j; d, h)$ is the complex signals at Tx-Rx separation distance d and the AP height h, $f_i(i = 1 \cdots M)$ is the observed M discrete frequency points, $t_j(j = 1 \cdots N)$ represents the N snapshots. The $g_{ant}(\theta, \varphi)$ is the antenna gain at elevational angle θ and azimuthal angel φ shown in Fig. 2(b) and Fig. 2(c). Two angels are calculated by $\theta = 2\pi - arcsin(\frac{d_{Bias}}{d_{ground}})$, $\varphi = 2\pi - arcsin(\frac{h}{d_{ground}})$ respectively, where the d_{ground} represents the horizontal distance between the wood stand and wearable antenna and d_{Bias} represents the shortest horizontal distance between the measured path and the wearable antenna.

The reference path loss $PL(d_0)$ is the initial path loss value at the reference distance $d_0 = 1$ m, including antenna gains. The PLE function $N(h)$ is first viewed as a constant n to evaluate the overall PLE parameter of the proposed off-body path loss model.

The measured 7,433,280 complex frequency response signals are fitted with the least square (LS) method. Fig. 3 shows recorded data and LS fitting path-loss curve. The overall PLE $n = 2.361$, is comparable to the path loss exponents of typical indoor environment found by empirical, numerical and analytical methods reported in [26]. Fig. 4 shows the probability distribution of shadow variable. The shadow variable X_δ conforms to zero mean Gaussian distribution with a standard deviation of 2.42 dB, close to [27]. Table 3 summarizes the parameters of the proposed path loss model.

These results show that the path loss model with the constant PLE fits well with the observed data. However, the AP height is proved to have a significant effect on the propagation prediction among various scenes [11]–[13], [17], [18], which are rarely report in BCC. The channel model for BAN in [13] shows that when the height of Rx changes from 0.25 to 1 m, the path loss value increases by 6.4 dB (from 54.7 to 62.2 dB) at the frequency band of 7.25-8.5 GHz. Similarly, when Rx is elevated from 1 to 2 m, the path loss increases by 5 dB for LOS case and 15 dB for NLOS one under in stair environment [17], [18]. As both the above scenes are measured with the Tx and Rx placed on wooden stand, the impact of height variation will be greater if the antenna is worn on human body. Thus, the height relevant studies are expected to further improve the predictive accuracy.

B. FITTING AND VALIDITY FOR PLE FACTOR

Fig. 5 shows five fitted path loss curves with different AP heights by the log-distance path loss model. It is clearly seen that the path loss is height-dependent. It is also supported by the improved 30 percent of the maximum likelihood values (MLH) during the path-loss fitting performance using the definite AP height observations other than the mixed height data.

Fig. 6 shows the fitted quadratic curve and the observed PLE values. The least square estimation approach and different functions, including power functions, logarithmic function and exponential function etc., are employed to model the path loss. It is found the quadratic function exhibits the

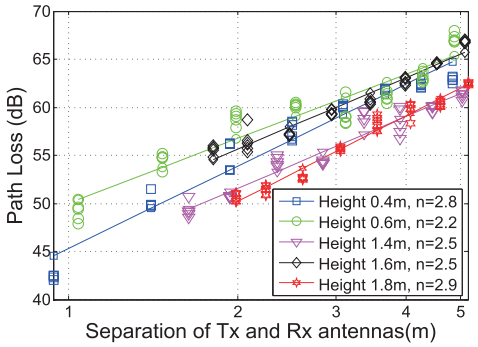

FIGURE 5. Comparison of five fitted path-loss curves at different AP heights and their distinctive PLE values.

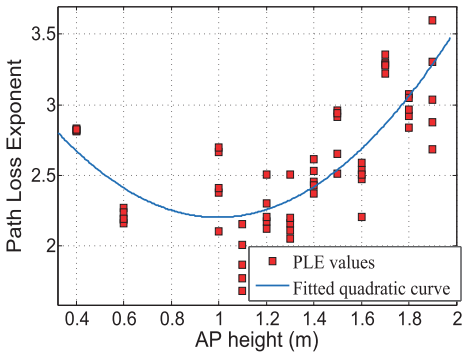

FIGURE 6. PLE factor values at various AP heights and the best fitted quadratic function.

best fitting performance. Table 3 lists the parameters for PLE function (2).

The well fit of the quadratic function on the height-dependent PLE factor $N(h)$ can be explained by the two-ray model and quasi free space propagation in specific indoor environment from the respects of the PLE bonds [11], [12]. The two-ray model reaches the maximum PLE value, when the distance between Tx and Rx antennas d is far enough shown as:

$$d \gg \sqrt{h_t h_r} \tag{4}$$

where h_t and h_r separately represent the heights of Tx and Rx [10]. Then, the path loss model will be simplified to:

$$PL_{two-ray}(d) = 40log_{10}(d) - 20log_{10}(h_t h_r) \tag{5}$$

where $PL_{two-ray}(d)$ is the path loss value of two ray model at distance d. Equation (5) shows the upper bound of PLE values for the two-ray model, i.e., PLE $n = 4$.

Fig. 7 shows the cross-sectional view of the AP height-dependent PLE factor under the hospital environment. The left part shows four AP locations at different heights and the same Tx-Rx separation distance $d = 5$ m. The four access points (APs) are the locations near the floor (i.e., Tx1), at the same height with bed (i.e., Tx2), in the middle of the room (i.e., Tx3), and close to the ceiling (i.e., Tx4). The coordinate axes on the right part of Fig. 7 shows a quadratic PLE

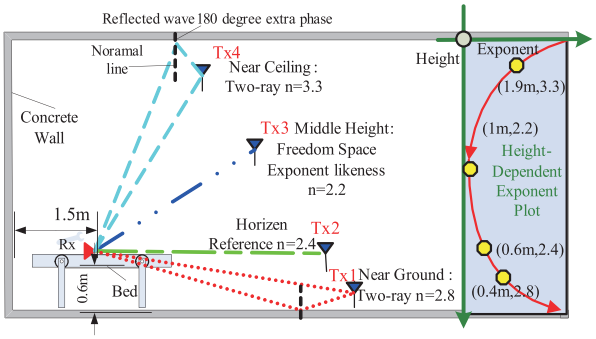

FIGURE 7. Cross-sectional view of AP height-dependent PLE factor and corresponding quadratic path-loss exponent function.

curve corresponding to the indoor AP height. Four circles in the PLE-height curve in the right part separately represent the specific PLE values of four APs on the left.

For Tx3 and Tx2 in Fig. 7, the PLEs of middle heights can be approximately explained by free space propagation PLE $n = 2$. The reflected components are much weaker than the direct ray, as the AP for Tx3 at the centre of the room is far away from the ground, ceiling and walls. For the APs like Tx2 around the bed-height, the shortest reflected path is blocked by the iron bed and the lying human body. This weakens the power of the reflected waves to 8-10dB less than the direct path in real measurement, similar to the UWB bed-shadowing report in [28]. The strongest direct path dominates the propagation characteristic in the moderate-height cases. As a result, the values of PLE are approximate to 2.

For Tx4, the PLE values of APs near the ceiling could be validated by the two-ray model. According to the two-ray model, in both cases the reflected ray has the almost same magnitude but the opposite phase with the direct ray [10]. Thus, the direct ray tends to be greatly weakened by the reflected ray in these cases. PLEs for Tx4 is 3.3, close to the upper bound PLE $n = 4$ in two-ray model (5).

Different from other APs which are higher than the bed, both the direct path and reflected waves of AP at Tx1 are greatly weakened by the iron bed and the lying body. There is less offset between direct path and shortest reflected wave, while abundant surface waves around the body makes the PLE slightly fluctuate among 2.4-2.8. Thus, PLE values are expected to mainly fluctuate between 2 and 4. PLE $n = 2$ is obtained under the free space fading and PLE $n = 4$ is the upper bound for two-ray model. This is in agreement with the observed PLE values and the fitted curve in Fig. 6 which range from 2.0 to 3.5. Due to the strong interference from the nearby reflectors, the PLE for the top or low Tx is greater than the medium height one under the same receiving conditions.

The analysis above implies that the quadratic fitting curve of PLE factor $N(h)$ is explained by the two-ray model and free space theory from the perspectives of symmetry and boundaries, especially when the APs are higher than the bed.

Fig. 8 shows the fitting surface of the two path loss models. As observed, it is clearly demonstrated that the

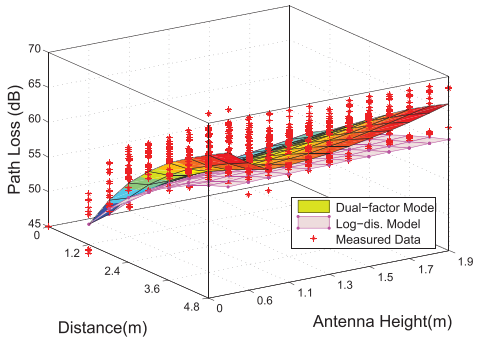

FIGURE 8. Simulation for the proposed height-dependent path-loss model on the left wrist under the NBO case.

TABLE 4. Comparison of various path loss models among mathematical express and goodness of fit.

Model cases		Mathematical express	RMSE
Overall	All data	$PL_0 + 10nlog_{10}(d/d_0)$	2.72
Height divided Models	Height 0.4m	$PL_0 + 10nlog_{10}(d/d_0)$	1.63
	Height 0.6m		1.79
	Height 1.4m		1.62
	Height 1.6m		1.08
	Height 1.8m		1.44
Height dependent Models	log-distance height gain model	$PL_0 + 10nlog_{10}(d/d_0) + alog_{10}(h/b)$	2.45
	Proposed model	$PL_0 + 10(ah^2 + bh + c)log_{10}(d/d_0)$	2.26

proposed model exhibits better fitting performance than the conventional log-distance height gain factor model with model shown in Table 4. The parameters for log-distance height gain model are PLE $n = 2.42$, $a = -2.48$ and $b = 4.47$. The deviation between the measured PLEs and predicted values by the proposed model is smaller than 2 dB, while the deviation between the measured PLEs and predicted values with log-distance model rise dramatically to more than 7 dB as the AP height and Tx-Rx distance increase. In this way, the accuracy of the dual-factor off-body model is both numerically and experimentally validated, and its novelty and effectiveness is also convinced.

In order to identify the appropriate path loss models for application, three kinds of models where evaluated in terms of root mean square errors (RMSE) are shown in Table 4. PL0 represents the reference path loss equivalent to PL(d0) and the fitted curves for three models are shown in Fig.3, Fig. 5 and Fig. 8. The root mean square of the differences between observed and predicted data sets is a meaningful measure of the error shown as:

$$RMSE = \sqrt{\frac{\sum_{i=1}^{n}(X_{obs,i} - X_{model,i})^2}{n}} \quad (6)$$

where $X_{obs,i}$ and $X_{model,i}$ are the observed and predicted values respectively. The number of two data sets are both n.The biggest RMSE value is with the overall (i.e. height-mixed) model while the most accurate kind of model is height divided modes with RMSE less than 1.5. However, this kind of models has an obvious shortcoming that repeated measurement and fitting are needed whenever the the AP height changes. Thus, the unified model (e.g. the height-dependent models) that takes the height factor into consideration is developed for convenience in application and link evaluation at the cost of prediction accuracy. Both the two height dependent models have 3 fitting parameters and their accuracies are better than overall model while inferior to height divided models from the perspective of RMSEs.

The proposed height-dependent PLE factor model is chosen mainly for three reasons. First, the constant PLE in the log-distance model is not reasonable when comparing to the fitted curves of height divided models with PLEs ranging from 2.2-2.9. In contrast, the PLE factor in the proposed model varies with the AP height. Second, in the BCC or body area network (BAN), the studies for PLE in different height not only improve the predictive accuracy but also provide more physical insight for AP deployment and system-level simulation. For tens or hundreds of APs in the future off-body communication, it is meaningful to reduce the power of APs with small PLE at the optimized height to reduce possible mutual interference. Last but not least, there are increasing modified attenuation factors for path loss model in off-body communication due to the body shadowing and antenna-body effect. Thus, it will benefit the extraction and analysis of body related attenuation factors to put those intrinsic parameters (e.g. height) into intrinsic part PLE.

The theoretical analysis and numerical simulation of PLEs imply that the novel off-body PLE factor is well characterized by the AP-height-dependent quadratic function.

C. EFFECT OF ANTENNA MISMATCH

As the polarization alignment between the Tx-Rx antennas is easy to be changed in off-body communication (e.g. the subject's small deflection, slight wrinkle of textile antennas and Tx-Rx inclination), the analysis of Tx and Rx mismatch on the accuracy of path loss model validation experience is very important. Figure 9 shows the Path loss fitted curves for measured case without polarization mismatch, Rx polarization direction changed and Tx polarization direction changed cases at the Tx height of 1 m and Rx worn on the left wrist. Under the same conditions, the PLEs over three scenes are all around 2.5. It seems that the polarization mismatch has no significant effect on the PLE values.

There are three main reasons. First, the dipole wideband wearable antennas adopted in this work have high cross polarization levels shown in Fig. 2(b) and Fig. 2(c). On one hand, the cross polarization components for dipole antenna are strong, as the cross polarized direction is perpendicular to the co-polarized direction shown in following figure (not included in the paper). On the other hand, the cross

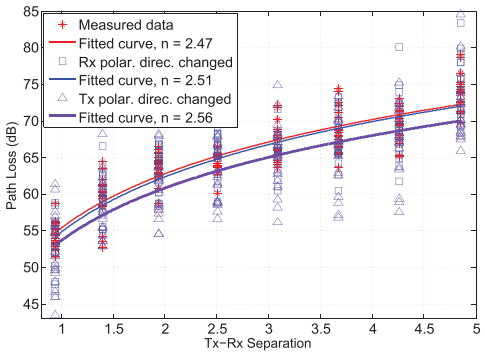

FIGURE 9. Path loss fitted curves for measured case without polarization mismatch, Rx polarization direction changed and Tx polarization direction changed cases at the Tx height of 1 m and Rx worn on the left wrist.

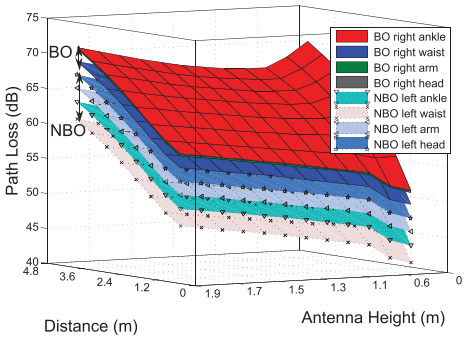

FIGURE 10. Simulation for the proposed dual-factor path-loss model (The top four surfaces for BO cases and the others for the BO).

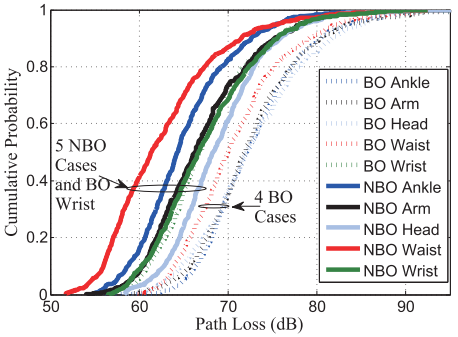

FIGURE 11. Comparison of measured path-loss data under both NBO and BO cases with the Tx-Rx separation is 3.6 m and the height of AP is 1.9 m.

polarization level for the wideband antennas is general high (see [29, Figs. 4–6]). Thus, the Rx can receive signals with cross polarized components. Second, the multipath components are complex under the indoor environment especially for off-body communication. Meanwhile, the polarization direction for the multipath components can be arbitrary [30]. Last but not least, the antennas for mobile applications are characterized by high cross polarized components (see [31, Figs. 12 and 13]) to guarantee that Users can receive signals in any polarized direction. Thus, the possible fading caused by polarization mismatch is made up by the high cross polarization of Rx and the complex multipath environment can provide an explanation.

D. MODELING AND VALIDATION OF BO FACTOR

Fig. 10 shows the systematic simulated surfaces of the dual-factor path-loss base on the height-dependent path-loss model in Fig. 8. The fitting path-loss surfaces under BO cases are evidently higher than the NBO ones while the disparity among the NBO path-loss surfaces (about 8 dB) are larger than the difference among the BO cases (about 3dB). It is seen that the introduction of the BO factor will further improve the accuracy of the proposed height-dependent model. For example, the dual-factor model provides 8 accurate path-loss values (60-67 dB for NBO cases and 68-70 for BO cases) for different body-worn parts while the traditional log-distance model in Fig. 8 provide only 58 dB (63dB provided by the height-dependent model) for general conditions with the same AP height of 1.9 m and Tx-Rx separation of 3.6 m.

Fig. 11 shows the cumulative probability distribution (CDF) of ten typical body-worn positions, i.e., head, arm, wrist, waist and ankle under the BO and NBO cases. The path-loss values of BO cases are generally 3 to 5 dB higher than the NBO ones due to the obstruction of human body [14]. Except for the wrist position, the other path-loss CDF curves for BO cases gather a cluster and the path-loss values generally increased by about 3dB compare to the NBO cases. Eighty percent of measured data under NBO cases ranges from 55 to 75 dB, while the BO cases are between 65 and 80 dB. In the aforementioned example, the interval from 60 to 70 dB clusters the most observed data which proves the accurate prediction of the dual-factor model. As the wide range of the path-loss distribution and the evident distinctions between BO and NBO cases, it is reasonable to depict ten scenarios with statistical parameters.

Fig. 10 and Fig. 11 show that from the perspective of link stability, wrist is the best body-worn position as the dissimilarity between NBO and BO cases is slight. Whilst, the strongest signal level case is the waist position under the NBO case despite the BO case for such position has an average of 8 dB signal drops.

Table 5 tabulates the log-normal distribution of path loss values for the proposed ten body-worn positions using maximum likelihood estimation (MLE) method. The MLEs and small deviation imply that the log-normal distribution depicts the off-body signal level well.

From the measured and fitted six parameters, i.e., log-normal fit of the signal level, root mean square (RMS) delay spread, mean delay, multi-path and coherent bandwidth with the method reported in [20], it is found that there are obvious differences among parameters of different body-worn positions and noticeable gaps between BO and NBO cases. For example, the multi-path parameters range from 75 main components to 139 for 5 body-worn parts under NBO situation and the components for NBO situation double the number for BO cases. The creeping waves around human body and reflections from torso and surroundings provide an

TABLE 5. Comparison of parameters on different body parts (Tx-Rx distance 3.06m).

Cases	Body-worn position	Lognormal Fit of Signal Level		RMS	Mean Delay	♯ of	Coherent Bandwidth
		Exp(μ) [dB]	σ	[ns]	[ns]	Multipath	[MHz]
NBO	Ankle	64.9	0.08	6.93	16.4	108	21.9
	Wrist	67.3	0.09	6.16	14.6	100	76.6
	Waist	62.4	0.10	5.32	13.8	80	58.3
	Arm	66.9	0.09	6.04	17.8	139	32.9
	Head	68.8	0.08	0.77	9.79	75	90.5
BO	Ankle	72.7	0.08	6.98	20.97	260	18.9
	Wrist	67.4	0.09	6.68	17.43	169	18.9
	Waist	70.7	0.08	4.97	19.31	307	14.6
	Arm	72.4	0.09	5.10	22.93	212	24.8
	Head	72.6	0.09	17.29	29.02	435	8.1

explanation for the differences between BO and NBO cases [32], [33]. Thus, it is necessary to introduce the BO factor to discriminate the BO and NBO cases caused by the body obstruction effect.

The analysis above implies that it is of great flexibility and accuracy to predict the path loss values under the off-body channel to introduce the BO factor dependent on the body-worn position and the PLE factor dependent on the AP height.

V. CONCLUSION

In this paper, a novel statistical path loss model with an AP height-dependent factor and a BO attenuation factor for off-body channel under hospital environment at 6-8.5GHz is developed and validated. The proposed model can provide not only the accurate off-body propagation prediction, but also the beneficial reference for the best antenna-height and body-worn-location deployment. Compare to the traditional log-distance path loss model, the proposed dual-factor model is observed an improvement of as high as 7dB under the condition of high AP deployment. In addition, the proposed model can be easily implemented in engineering and extended to other height-related scenarios, due to its clear physical insights of the two factors. Therefore, it is a promising candidate model in future developments of novel physical layer transmission schemes in the BCC systems.

As large amounts of electronic devices which have a high link reliability and stringent electromagnetic safety requirement have been employed in the hospital environment, our future work will focus on the challenging problems of multi-device coexistence and reliable off-body communication links.

ACKNOWLEDGMENT

The authors wish to thank Ms. Man You, Ms. Bai Xue, Ms. Ling Li, Mr. Ji Zhang, Mr. Hua-Quan Yang and Mr. Chun-Rui Guo, Nanjing University of Posts and Telecommunications, for their help and assistance in the off-body channel measurement.

REFERENCES

[1] T. Wang, G. Li, J.-X. Ding, Q.-Y. Miao, J.-C. Li, and Y. Wang, "5G spectrum: Is China ready?" *IEEE Commun. Mag.*, vol. 53, no. 7, pp. 58–65, Jul. 2015.

[2] P. Pirinen, "A brief overview of 5G research activities," in *Proc. 1st Int. Conf. 5G Ubiquitous Connectivity*, 2014, pp. 17–22.

[3] S. J. Ambroziak, L. M. Correia, and R. J. Katulski al, "An off-body channel model for body area networks in indoor environments," *IEEE Trans. Antennas Propag.*, vol. 64, no. 9, pp. 4022–4035, Sep. 2016.

[4] P. Hall and Y. Hao, *Antennas and Propagation for Body-Centric Wireless Communications* (Antennas and Propagation Library), 2nd ed. Norwood, MA, USA: Artech House, 2012.

[5] R. G. Garcia-Serna, C. Garcia-Pardo, and J. M. Molina-Garcia-Pardo, "Effect of the receiver attachment position on ultrawideband off-body channels," *IEEE Antennas Wireless Propag. Lett.*, vol. 14, pp. 1101–1104, 2015.

[6] S. V. Roy *et al.*, "Dynamic channel modeling for multi-sensor body area networks," *IEEE Trans. Antennas Propag.*, vol. 61, no. 4, pp. 2200–2208, Apr. 2013.

[7] M. M. Khan, Q. H. Abbasi, A. Alomainy, and Y. Hao, "Experimental characterisation of ultra-wideband off-body radio channels considering antenna effects," *IET Microw. Antennas Propag.*, vol. 7, no. 5, pp. 370–380, May 2013.

[8] D. Smith *et al.*, "Characterization of the dynamic narrowband on-body to off-body area channel," in *Proc. IEEE Int. Conf. Commun.*, Jun. 2009, pp. 1–6.

[9] A. Taparugssanagorn, C. Pomalaza-Rez, and R. Tesi, "UWB channel for wireless body area networks in a hospital environment," *Int. J. Ultra Wideband Commun. Syst.*, vol. 1, no. 4, pp. 226–236, 2010.

[10] T. S. Rappaport, "Mobile radio propagation: Large-scale path loss," in *Proc. Wireless Commun. Principles Pract.*, 2008, pp. 41–58.

[11] R. E. Badra and A. Zambrano, "Street-level LOS/NLOS model for urban macrocells based on observations," in *Proc. IEEE Wireless Commun. Netw. Conf.*, Mar. 2011, pp. 1294–1297.

[12] M. Zhao *et al.*, "A two-dimensional integrated channel model for train-ground communications," in *Proc. 21st Int. Conf. Telecommun. (ICT)*, Dec. 2014, pp. 348–352.

[13] *Channel Model for Body Area Network Working Group for Wireless Personal Area Networks*, IEEE P802.15-08-0780-09-0006, New York, NY, USA, Apr. 2009.

[14] P.-F. Cui, Y. Yu, Y. Liu, W.-J. Lu, and H.-B. Zhu, "Body obstruction characteristics for off-body channel under hospital environment at 6 8.5 GHz," *IEEE Int. Conf. Ubiquitous Wireless Broadband*, Oct. 2016, pp. 1–4.

[15] S. L. Cotton and W. G. Scanlon, "Channel characterization for single- and multiple-antenna wearable systems used for indoor body-to-body communications," *IEEE Trans. Antennas Propag.*, vol. 57, no. 4, pp. 980–990, Apr. 2009.

[16] Q. N. Zhang, J. Zhang, D. Y. Zhang, W.-J. Lu, K. F. Tong, and H. B. Zhu, "A wearable loop-dipole combined antenna," in *Proc. Int. Workshop Electromagn.*, 2016, pp. 1–3.

[17] Y. Yu, Y. Liu, W.-J. Lu, and H.-B. Zhu, "Path loss model with antenna height dependency under indoor stair environment," *Int. J. Antennas Propag.*, vol. 2014, pp. 1-6, Jul. 2014.
[18] Y. Liu, Y. Yu, W.-J. Lu, and H.-B. Zhu, "Antenna-height-dependent path loss model and shadowing characteristics under indoor stair environment at 2.6 GHz," *IEE J. Trans. Elect. Electron. Eng.*, vol. 10, no. 5, pp. 498–502, May 2015.
[19] Y. Wang, W.-J. Lu, and H.-B. Zhu, "Propagation characteristics of the LTE indoor radio channel with persons at 2.6 GHz," *IEEE Antennas Wireless Propag. Lett.*, vol. 12, pp. 991–994, 2013.
[20] Y. Wang, W.-J. Lu, and H.-B. Zhu, "Study on multipath propagation characteristics for LTE indoor environment with persons," in *Proc. IEEE Int. Wireless Symp.*, Apr. 2013, pp. 1–4.
[21] P. S. Hall *et al.*, "Antennas and propagation for on-body communication systems," *IEEE Antennas Propag. Mag.*, vol. 49, no. 3, pp. 41–58, Jun. 2007.
[22] J. Hwng, T. Kang, Y. Kim, and S. Park, "Measurement of transmission properties of HBC channel and its impulse response model," *IEEE Trans. Instrum. Meas.*, vol. 65, no. 1, pp. 177–188, Jan. 2016.
[23] T. Mavridis, L. Petrillo, J. Sarrazin, D. Lautru, A. Benlarbi-Delai, and P. De Doncker, "Theoretical and experimental investigation of a 60-GHz off-body propagation model," *IEEE Trans. Antennas Propag.*, vol. 62, no. 1, pp. 393–402, Jan. 2014.
[24] M. S. Wegmueller, M. Oberle, N. Felber, N. Kuster, and W. Fichtner, "Signal transmission by galvanic coupling through the human body" *IEEE Trans. Instrum. Meas.*, vol. 59, no. 4, pp. 963–969, Apr. 2010.
[25] S. S. Ghassemzadeh, R. Jana, C. W. Rice, W. Turin, and V. Tarokh, "Measurement and modeling of an ultra-wide bandwidth indoor channel," *IEEE Trans. Commun.*, vol. 52, no. 10, pp. 1786–1796, Oct. 2004.
[26] H. Hashemi, "The indoor radio propagation channel," *Proc. IEEE*, vol. 81, no. 7, pp. 943–968, Jul. 1993.
[27] G. D. Durgin, T. S. Rappaport, and H. Xu, "Measurements and models for radio path loss and penetration loss in and around homes and trees at 5.85 GHz," *IEEE Trans. Commun.*, vol. 46, no. 11, pp. 1484–1496, Nov. 1998.
[28] K. Yamasue, Y. Obinata, K. Takizawa, C. Sugimoto, and R. Kohno, "Measures against shadowing problem on a bed using high-band UWB-BAN," in *Proc. Int. Workshop Electromagn.*, 2013, pp. 198–202.
[29] S. Choi, J. Park, K. Sun, and J. Park, "A new ultra-wideband antenna for UWB applications," *Microw. Opt. Technol. Lett.*, vol. 40, no. 5, pp. 399–401, 2004.
[30] Y. Add Ban, C. Li, C. Sim, and G. Wu, "4G/5G multiple antennas for future multi-mode smartphone applications," *IEEE Access*, vol. 4, pp. 2981–2988, 2016.
[31] A. Kajiwara, "Line-of-sight indoor radio communication using circular polarized waves," *IEEE Trans. Veh. Technol.*, vol. 44, no. 3, pp. 487–493, Aug. 1995.
[32] Q. H. Abbasi, A. Sani, A. Alomainy, and Y. Hao, "On-body radio channel characterization and system-level modeling for multiband OFDM ultra-wideband body-centric wireless network," *IEEE Trans. Microw. Theory Techn.*, vol. 58, no. 12, pp. 3485–3492, Dec. 2010.
[33] Y. Zhao, Y. Hao, A. Alomainy, and C. Parini, "UWB on-body radio channel modeling using ray theory and subband FDTD method," *IEEE Trans. Microw. Theory Techn.*, vol. 54, no. 4, pp. 1827–1835, Jun. 2006.

PENG-FEI CUI was born in Yancheng, China, in 1990. He received the B.E. degree in electrical engineering from Soochow University, Suzhou, China, in 2013. His research interests include body-centric communication, wireless channel measurement, and channel modeling.

YU YU was born in Nanjing, China, in 1990. He received the B.E. degree in electrical engineering from Nanjing University of Posts and Telecommunications, Nanjing, China, in 2012. He has authored or co-authored more than ten research papers in peer-reviewed international journals and conference proceedings. His research interests include wireless propagation and wireless channel modeling.

WEN-JUN LU (M'12) was born in Jiangmen, China, in 1978. He received the B.E. and Ph.D. degrees in communication engineering and electrical engineering from Nanjing University of Posts and Telecommunications (NUPT), Nanjing, China, in 2001 and 2007, respectively. He was a Lecturer (2007–2009), an Associate Professor (2009–2013), and has been a Professor (since 2013) with the Jiangsu Key Laboratory of Wireless Communications, NUPT. He has authored or co-authored more than 120 technical papers published in peer-reviewed international journals and conference proceedings. He is the Translator of the Chinese version of *The Art and Science of Ultra Wideband Antennas* (by H. Schantz). He has authored the book *Antennas: Concise Theory, Design and Applications* (in Chinese). His research interests include antenna theory, and wideband antennas and arrays. He has been serving as an Editorial Board Member of the *International Journal of RF and Microwave Computer-Aided Engineering* since 2014. He received the Exceptional Reviewers Award of the IEEE TRANSACTIONS ON ANTENNAS AND PROPAGATION in 2016, the Award of New Century Excellent Talents in Universities from the Ministry of Education of China in 2012, and the Nomination Award of Top-100 Outstanding Ph.D. Dissertation of China in 2009. He was also a co-recipient of six scientific and technological awards granted by the Jiangsu Province, the Chinese Institute of Electronics, and the Chinese Institute of Communications.

YANG LIU was born in Wuxi, China, in 1988. He received the B.E. and Ph.D. degrees in electrical engineering from Nanjing University of Posts and Telecommunications, Nanjing, China, in 2010 and 2016, respectively. He has been a Lecturer with Jiangnan University, Wuxi, China, since 2016. He has authored or co-authored more than research papers in peer-reviewed international journals and conference proceedings. His research interests include wireless propagation and wireless channel modeling.

HONG-BO ZHU was born in Yangzhou, China, in 1956. He received the Ph.D. degree in electrical engineering from Beijing University of Posts and Telecommunications, China, in 1996. He was the Vice President of Nanjing University of Posts and Telecommunications from 2008 to 2016, where he is currently the Director of the Jiangsu Key Laboratory of Wireless Communications. He has authored or co-authored more than 300 research papers in peer-reviewed international journals and conference proceedings. He is the primary Inventor and a Co-Inventor of more than 60 granted Chinese patents. His research interests include wireless communications theory and Internet of Things. He is a Fellow of the Chinese Institute of Electronics and a Fellow of the Chinese Institute of Communications. He was a co-recipient of the Best Paper Award of Global-Com 2016. He is also the leading recipient of eight scientific and technological awards granted by the Jiangsu Province, the Chinese Institute of Electronics, and the Chinese Institute of Communications.